Electronic Supplementary Information (ESI)

Silicon-supported 2D conductive metal-organic framework nanorod arrays for alkaline water and urea electrooxidation

Supattra Somsri,[a,b] Phirom Boun,[a,b] Tai Le-Thanh,[a,b] Sébastien Bonhommeau,[a] David Talaga,[a] Véronique Lapeyre,[a] Bertrand Goudeau,[a] and Gabriel Loget*[a] and Ie-Rang Jeon*[b]

[a.] Univ. Bordeaux, CNRS, Bordeaux INP, ISM, UMR 5255, F-33400 Talence, France.
[b.] Univ. Bordeaux, CNRS, CRPP, UMR 5031, F-33600 Pessac, France.

*Corresponding authors: gabriel.loget@cnrs.fr, ie-rang.jeon@crpp.cnrs.fr

Table and Contents

1. Materials and experiments

1.1 Materials

The following reagents were used as received without further purification. Iron(III) chloride ($FeCl_3$, anhydrous, ≥97%), sulfuric acid (H_2SO_4, 95 - 98%), hydrobromic acid (HBr, 33% w/w in acetic acid), dichloromethane (CH_2Cl_2, ≥99.8%), glacial acetic acid (CH_3COOH, ≥99.8%), nickel(II) acetate tetrahydrate ($Ni(CH_3COO)_2{\cdot}4H_2O$, 98%), sodium acetate trihydrate ($NaCH_3COO{\cdot}3H_2O$, ≥99%), potassium hydroxide (KOH, 90%), and urea were all purchased from Sigma-Aldrich. Acetone was acquired from J.T. Baker. Absolute ethanol and methanol were obtained from VWR. Hydrogen peroxide solution (H_2O_2, 30% w/w in H_2O) was supplied by Honeywell. Degenerate boron-doped p^{++}-type silicon wafers (single-side polished, (100) orientation, resistivity 0.001 - 0.005 Ω·cm, thickness 500 ± 10 µm) were purchased from Latech Scientific Supply. Ultrapure water (resistivity ≥ 18.2 MΩ·cm) was used throughout all experiments.

1.2 Synthesis of 2,3,6,7,10,11-hexahydroxytriphenylene (H_6HHTP)

The synthetic route to the triphenylene core proceeded in two steps, beginning with oxidative trimerization of veratrole to afford 2,3,6,7,10,11-hexamethoxytriphenylene (HMTP, **1**), followed by complete ether cleavage to yield the target hexahydroxytriphenylene (**2**), following an adapted literature procedure.[1-3]

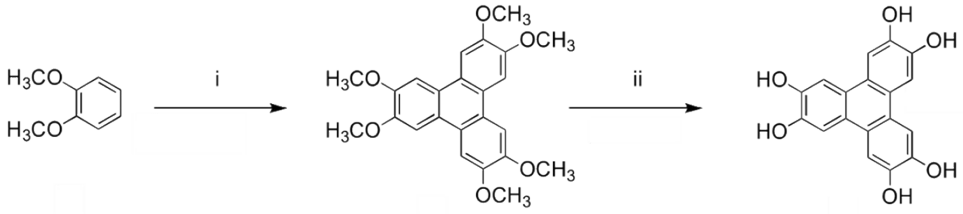

veratrole HMTP (**1**) H_6HHTP (**2**)

i. 2,3,6,7,10,11-hexamethoxytriphenylene (HMTP) (**1**)

A suspension of $FeCl_3$ (25.5 g, 0.157 mol) in anhydrous CH_2Cl_2 (150 mL) was treated with H_2SO_4 (0.35 mL). A solution of veratrole (6.91 g, 0.05 mol) dissolved in CH_2Cl_2 (70 mL) was introduced dropwise into the stirring mixture. The resulting black suspension was maintained at room temperature with continuous stirring for 3 h. Methanol (200 mL) was then introduced dropwise with caution due to the highly exothermic nature of this addition. Upon methanol addition, the dark suspension underwent a colour change to an orange-brown suspension. Stirring was continued at room temperature for an additional 30 minutes (min), after which the solid product was collected by filtration, washed thoroughly with MeOH (200 mL), and dried under ambient conditions to afford a beige powder. The crude product was carried forward to the next step without additional purification. Yield: 4.56 g (67%).

^{1}H NMR (400 MHz, $CDCl_3$, TMS): δ = 4.11 (s, 18H, $6CH_3$), 7.76 (s, 6H, ArH).

ii. 2,3,6,7,10,11-hexahydroxytriphenylene (H_6HHTP) (2)

A suspension of HMTP (**1**) (2.5 g, 6.1 mmol) in a mixture of HBr (33% w/w in acetic acid, 85 mL) and glacial CH_3COOH (85 mL) was degassed under a continuous flow of argon at

room temperature for 30 min, yielding a beige-coloured suspension. The mixture was subsequently heated under reflux for 12 h while maintaining an inert argon atmosphere, during which time the suspension darkened to grey. After allowing the reaction to cool to room temperature under argon, the precipitate was isolated by filtration, rinsed with cold deionized water, and dried under ambient conditions to give a pale grey powder. Yield: 1.85 g (93%).

^{1}H NMR (400 MHz, DMSO-d_6, TMS): δ = 7.60 (s, 6H, ArH), 9.27 (s, 6H, OH).

1.3 Preparation of Si/Ni

Prior to use, p^{++}-Si wafers underwent sequential ultrasonic cleaning in acetone, ethanol, and ultrapure water (10 min each), followed by drying under a stream of nitrogen. Surface oxidation was subsequently carried out by immersing the cleaned wafers in piranha solution at 105 °C for 30 min to generate a uniform SiO_x overlayer. Nickel thin films were then deposited onto the resulting p^{++}-Si/SiO_x substrates by magnetron sputtering using a Leica EM ACE600 coating system equipped with a Ni target of 99.8% purity. Deposition was performed under an argon atmosphere at a working pressure of 2 x10^{-2} mbar and an applied current of 100 mA. The growth of the film thickness (approximately 20 nm) was monitored continuously during deposition by an *in situ* quartz crystal microbalance (QCM). Upon completion of the deposition process, the chamber was purged with N_2.

1.4 Preparation of Si/Ni/Ni-HHTP

In a glass vial, $Ni(CH_3COO)_2{\cdot}4H_2O$ (15 mg, 0.06 mmol) was dissolved in ultrapure water (5 mL). H_6HHTP (10 mg, 0.03 mmol) was subsequently introduced into the solution as a solid, and the resulting mixture was sonicated at 45 kHz for 1 min to yield a homogeneous blue suspension. A Si/Ni substrate was then immersed in the suspension and the vial was transferred to an oven and maintained at 85 °C for 2 h. After cooling to ambient temperature for 60 min, the surface was carefully retrieved, rinsed thoroughly with ultrapure water, and dried under a stream of N_2 to afford the Si/Ni/Ni-HHTP thin-film electrode.

1.5 Preparation of Ni-HHTP powder

$Ni(CH_3COO)_2{\cdot}4H_2O$ (15 mg, 0.06 mmol) and $NaCH_3COO{\cdot}3H_2O$ (24 mg, 0.176 mmol) were dissolved in ultrapure water (5 mL) in a glass vial (25 × 45 mm). H_6HHTP (10 mg, 0.03 mmol) was added as a solid to the stirring solution, and the mixture was subjected to sonication for 1 min to produce a uniform blue suspension. The sealed vial was subsequently placed in an oven at 85 °C for 12 h then cooled to ambient temperature for 60 min. The resulting dark blue precipitate was isolated by filtration and sequentially washed with water, ethanol, and acetone to remove unreacted precursors and residual solvent. The solid was then dried under ambient conditions to give Ni-HHTP as a dark blue powder. Yield: 11.2 mg (90%).

1.6 Preparation of electrode

An ohmic contact was established on the rear face of the Si substrate using the following procedure. The back surface was first abraded with a diamond-tipped glass cutter to expose fresh silicon, onto which a small droplet of eutectic InGa alloy (99.99% metals basis, Alfa Aesar) was applied. A metal wire was embedded into the InGa layer, and the entire contact region was encapsulated with a layer of conductive silver paste (Conductive Silver, Electron

Microscopy Sciences) to secure the wire and ensure reliable electrical connection. Once the silver paste had dried, the rear face of the substrate together with the adjacent portion of the metal wire was sealed using an epoxy resin (Loctite 9460, Henkel) to electrically isolate the ohmic contact from the electrolyte. A defined geometric electrode area was simultaneously defined on the front face of the Si substrate using the same epoxy resin. The assembled electrode was cured in an oven at 90 °C for 1 h to achieve complete hardening of the resin.

2. Characterizations

Nuclear magnetic resonance (NMR) spectroscopy. ^{1}H NMR spectra were recorded on a JEOL JNM-ECS400 spectrometer (400 MHz) at 25 °C. Chemical shifts (δ) are reported in ppm relative to the residual solvent signal (DMSO-d_6: δ 2.50 ppm; $CDCl_3$: δ 7.26 ppm).

Scanning electron microscopy (SEM) images were collected using a Hitachi SU7000 field-emission scanning electron microscope at an accelerating voltage of 3.00 kV. Energy dispersive X-ray spectroscopy (EDX) elemental mapping was performed using a Bruker XFlash 760 detector with Esprit software at a primary beam energy of 15 keV.

Transmission electron microscopy (TEM) images were acquired using a JEOL JEM-2100 transmission electron microscope equipped with a Gatan Orius SC200D camera and operated at 200 kV.

Fourier-transform infrared (FT-IR) two FT-IR configurations were employed for spectral acquisition over 400–4000 cm^{-1}. Thin-film electrodes (Si/Ni and Si/Ni/Ni-HHTP) were measured in external specular reflectance mode on a Thermo Scientific Nicolet 6700 spectrometer equipped with a PIKE Technologies VeeMAX II accessory at a fixed angle of 50° (OMNIC software). The H_6HHTP ligand and bulk Ni-HHTP powder were measured in ATR mode on a Thermo Scientific Nicolet iS50 spectrometer. FTIR spectra are stacked with a vertical offset for visual comparison.

X-ray photoelectron spectroscopy (XPS) measurements were carried out on a K-Alpha spectrometer (Thermo Fisher Scientific) using a monochromatic Al Kα X-ray source operating at a photon energy of 1486.7 eV. The incident X-ray beam was focused to a spot diameter of approximately 400 μm on the sample surface. Survey spectra were acquired over a binding energy range of 0-1150 eV at a pass energy of 200 eV, and high-resolution core-level spectra were collected at a reduced pass energy of 40 eV to achieve improved energy resolution. All measurements were conducted with charge neutralization.

Powder X-ray diffraction (PXRD) patterns were collected using a Rigaku SmartLab diffractometer equipped with a Cu Kα radiation source (λ = 1.5406 Å) operating at 40 kV and 50 mA. Data were recorded in the 2θ range of 2°-50° with a step size of 0.02° and a scan speed of 1.0°/min, using a D/teX Ultra 250 1D silicon strip detector. Bulk Ni-HHTP powder was

mounted on a microscope slide for measurement, while Si/Ni/Ni-HHTP thin-film electrodes were measured directly without further sample preparation.

Raman spectra were collected using a HORIBA LabRAM spectrometer equipped with a 633 nm He-Ne laser and a Syncerity CCD detector. An a-Clipse electrochemical cell (Idylle Labs) was employed for the in-situ Raman spectroscopy. A ×50 objective, 600 gr/mm grating, and 10% laser power filter (laser power of 680 µW) were used. Spectra were recorded over the range 300–1800 cm^{-1} with 9 accumulations (total acquisition time: 4 min 12 s). Spectro-electrochemical experiments were carried out in four successive stages. First, the electrode was characterized as a dry sample using 1% laser power (55 µW) in the absence of electrolyte. The electrolyte was then introduced into the cell, and the electrode was allowed to equilibrate at open-circuit potential (OCP) for 5 min before acquisition as a wet sample using 10% laser power. A defined potential was subsequently applied for 5 min while Raman spectra were simultaneously recorded. The applied potential was then stepped incrementally in both anodic and cathodic directions, with spectra acquired at each step, before a final measurement was taken after returning to OCP.

Ion chromatography (IC) anion concentrations were determined by ion chromatography using a Thermo Scientific Dionex Inuvion IC system equipped with an electrolytic eluent generator and a conductivity detector, controlled by Chromeleon 7.3 software. Separations were carried out at a flow rate of 0.30 mL/min with a KOH eluent gradient (15–72 mM over 10 min), column temperature of 30 °C. The injection volume was 1 µL and the total run time was 21 min.

Electrochemical measurements were performed using a Biologic SP-50 potentiostat controlled by EC-Lab software. An Hg/HgO (1 M KOH) electrode and carbon rod were used as reference and counter electrodes. All potentials are referenced to the reversible hydrogen electrode (RHE). The Hg/HgO reference electrode (1 M KOH, $E^{\circ}_{Hg/HgO}$ = +0.098 V vs. NHE) was calibrated against the RHE scale using the following relation:

$$E_{RHE} = E_{Hg/HgO} + E^{\circ}_{Hg/HgO} + (0.0592 \times pH)$$

In 1 M KOH (pH = 14), this gives a total offset of +0.93 V, such that:

$$E_{RHE} = E_{Hg/HgO} + 0.93\ V$$

Calculation of Faradaic Efficiency (FE)

Determination of the theoretical charge from chronoamperometry

The theoretical charge $Q_{theoretical}$ (C) passed during the chronoamperometric experiment was calculated by integrating the current–time profile:

$$Q_{theoretical} = \int I(t)dt$$

where I is the applied current (A) and t is the elapsed time (s).

Quantification of products

The urea oxidation reaction (UOR) proceeds according to:[4]

$$CO(NH_2)_2(aq) + 8\ OH^-(aq) \rightarrow NCO^-(aq) + NO_2^-(aq) + 6\ H_2O(l) + 6\ e^- \quad (1)$$

Based on this stoichiometry, the oxidation of 1 mole of urea produces 1 mole of NO_2^- and 1 mole of NCO^-, producing 6 moles of electrons per mole of product formed. The molar amounts of NO_2^- and NCO^- were quantified by ion chromatography (IC) using a Thermo Scientific Dionex Inuvion system. The concentration of each species was determined from chromatographic peak area using external calibration curves spanning 0-120 µM (NO_2^-) and 0-148 µM (NCO^-) and converted to molar amounts using the known sample volume and dilution factor (Fig S8). The electrochemical reaction was carried out in 25 mL of a solution containing 0.33 M urea and 1 M KOH. Following the reaction, the solution was diluted 50-fold with ultrapure water prior to injection into the ion chromatography (IC) system. For calibration, standard solutions of KNO_2 were prepared in 1 M KOH at an initial concentration of 1200 µM, then diluted with ultrapure water by factors of 10, 20, 50, and 100 to yield concentrations of 120, 60, 24, and 12 µM, respectively. Similarly, standard solutions of NaOCN were prepared in 1 M KOH at 1480 µM and subsequently diluted by the same factors to give concentrations of 148, 74, 30, and 15 µM, respectively. All standard solutions were injected directly into the IC system without further treatment.

Experimental charge

The experimental charge required to produce the detected amount of NO_2^- was calculated as:

$$Q_{experimental} = {}^{n}_{NO_2^-} \times 6 \times F \quad (1)$$

where ${}^{n}_{NO_2^-}$ is the molar amount of NO_2^- detected (mol), 6 is the number of electrons produced per urea molecule, and F is the Faraday constant (96485 C mol^{-1}).

Faradaic efficiency

The Faradaic efficiency (FE) for reaction (1) production was then determined as:

$$FE\ (\%) = \frac{Q_{experimental}}{Q_{theoretical}} \times 100 = \frac{{}^{n}_{NO_2^-} \times 6 \times F}{Q_{theoretical}} \times 100$$

3. Supplementary figures and table

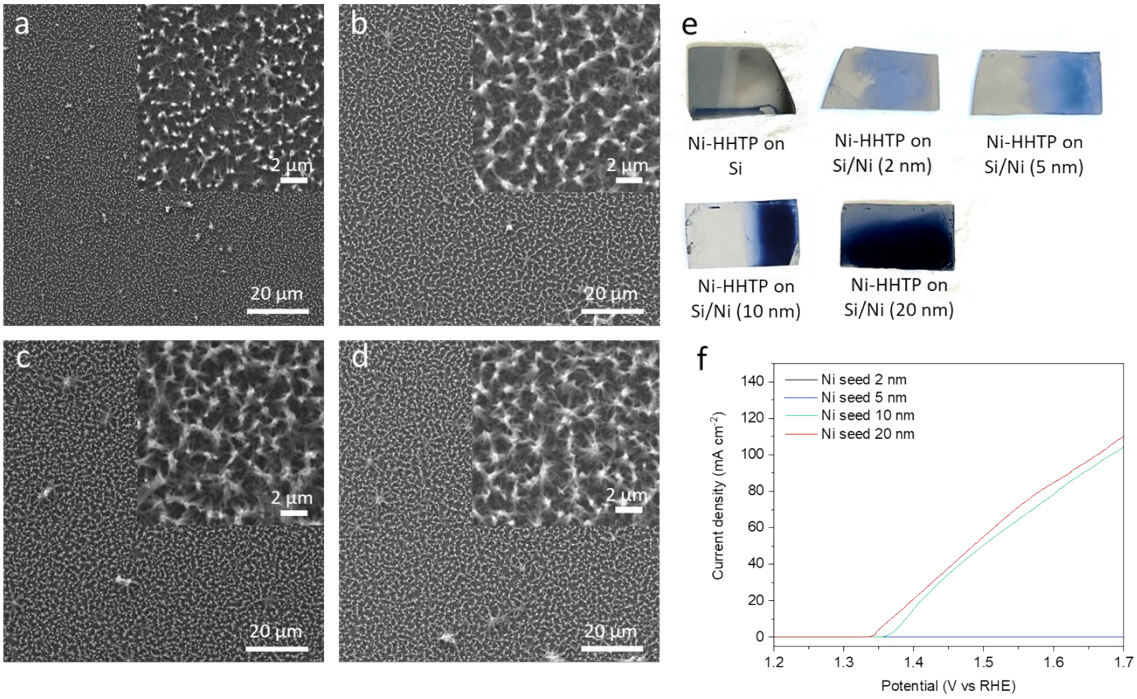

Figure S1. SEM images of Si/Ni/Ni-HHTP when Ni thin film is (a) 2 nm, (b) 5 nm, (c) 10 nm and (d) 20 nm. (e) Pictures of Ni-HHTP growth on Si, Si/Ni 2 nm, Si/Ni 5 nm, Si/Ni 10 nm and Si/Ni 20 nm. (f) LSVs of Si/Ni/Ni-HHTP recorded in 0.33 M urea + 1 M KOH. The 20 nm Ni interlayer was selected as optimal because it provides sufficient nucleation sites for complete and uniform Ni-HHTP MOF film formation, resulting in the lowest onset potential (1.33 V vs. RHE) and highest current density (110 mA cm^{-2} at 1.7 V) for urea oxidation.

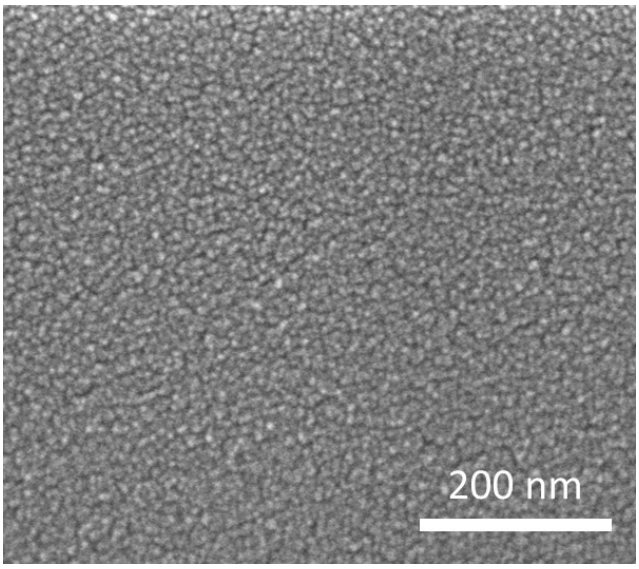

Figure S2. High resolution SEM image of Si/Ni.

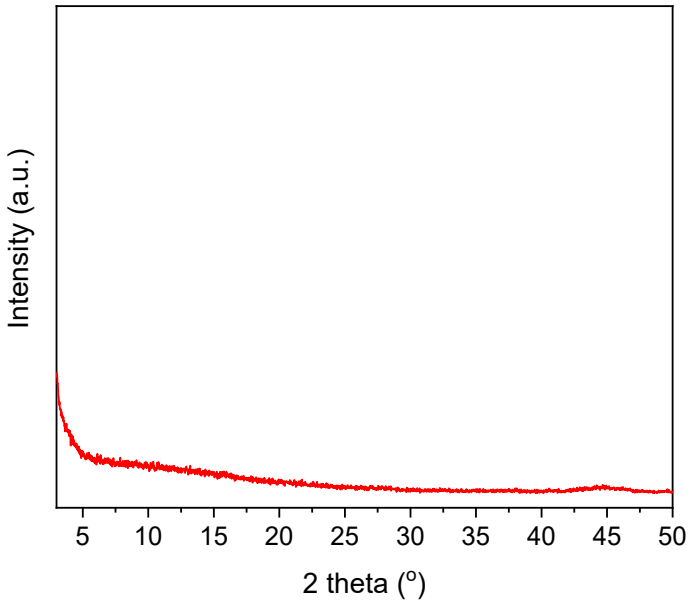

Figure S3. Thin-film XRD of Si/Ni.

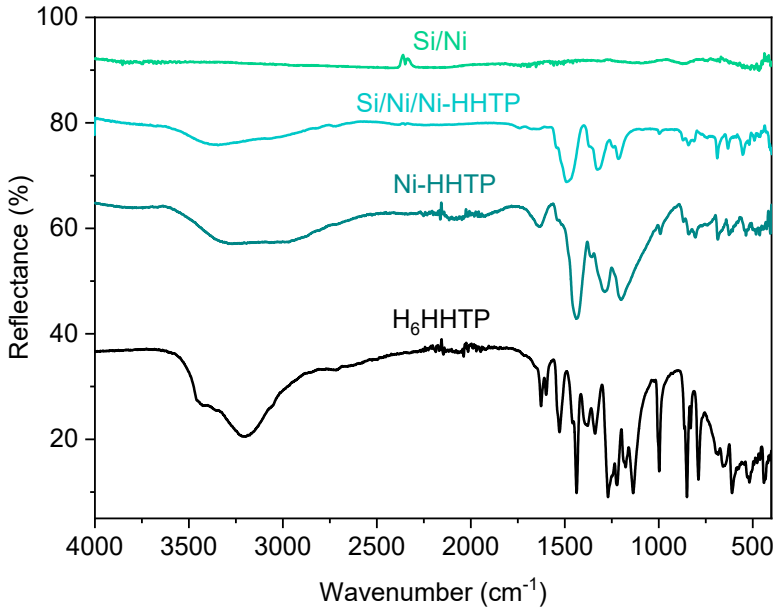

Figure S4. FT-IR spectra of H_6HHTP, Ni-HHTP powder, Si/Ni/Ni-HHTP, and Si/Ni.

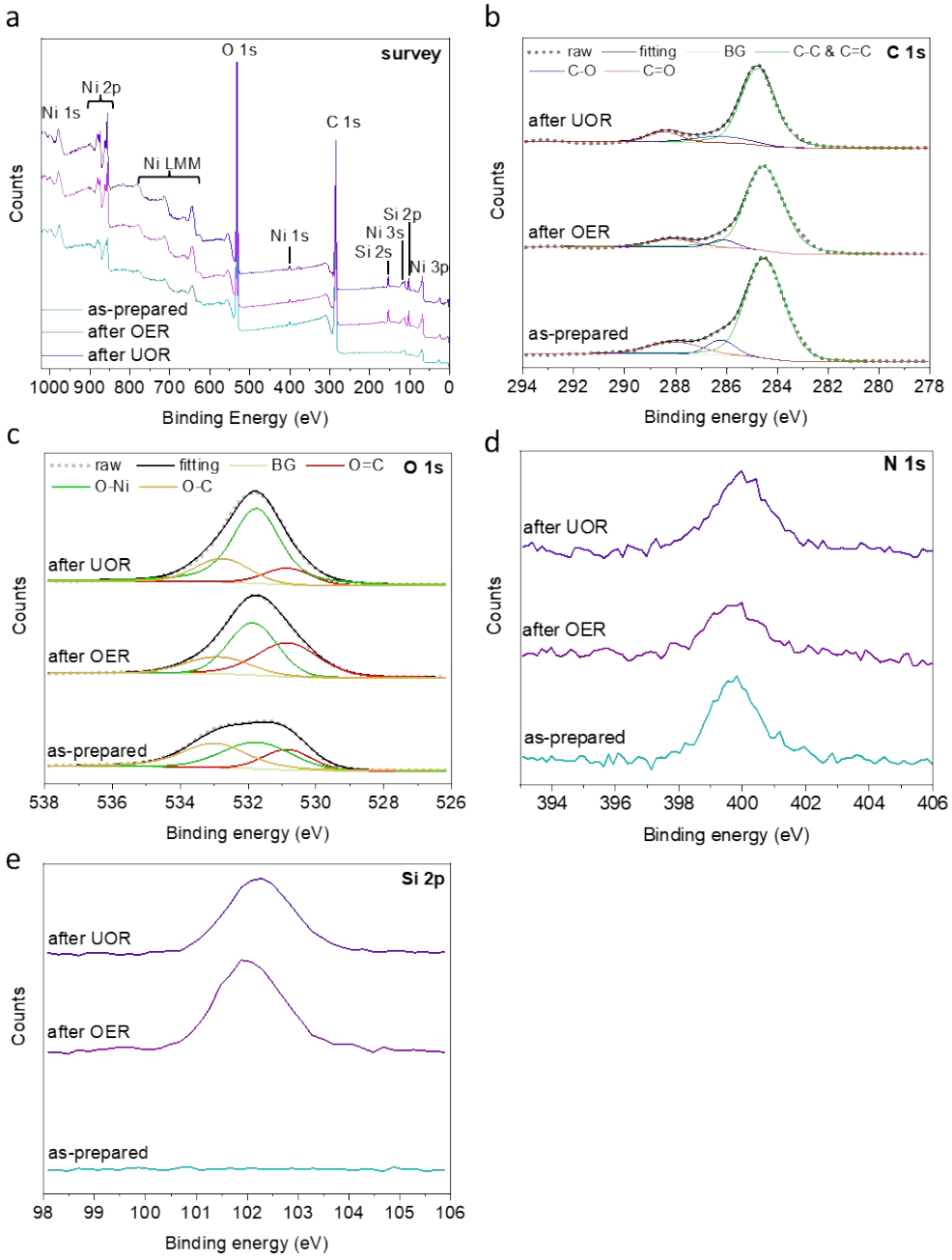

Figure S5. XPS spectra of Si/Ni/Ni-HHTP: as-prepared, after OER and after UOR (a) XPS survey, (b) C 1s (c) O 1s, (d) N 1s and (e) Si 2p.

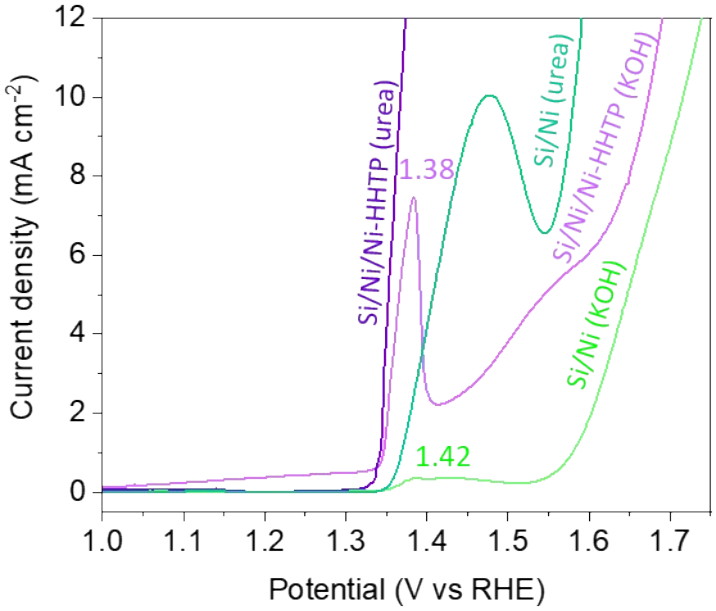

Figure S6. LSVs recorded in 1 M KOH and 0.33 M urea + 1 M KOH with Si/Ni and Si/Ni/Ni-HHTP, showing characteristic Ni^{2+}/Ni^{3+} redox couple at 1.42 and 1.38 V vs. RHE for Si/Ni and Si/Ni/Ni-HHTP, respectively.

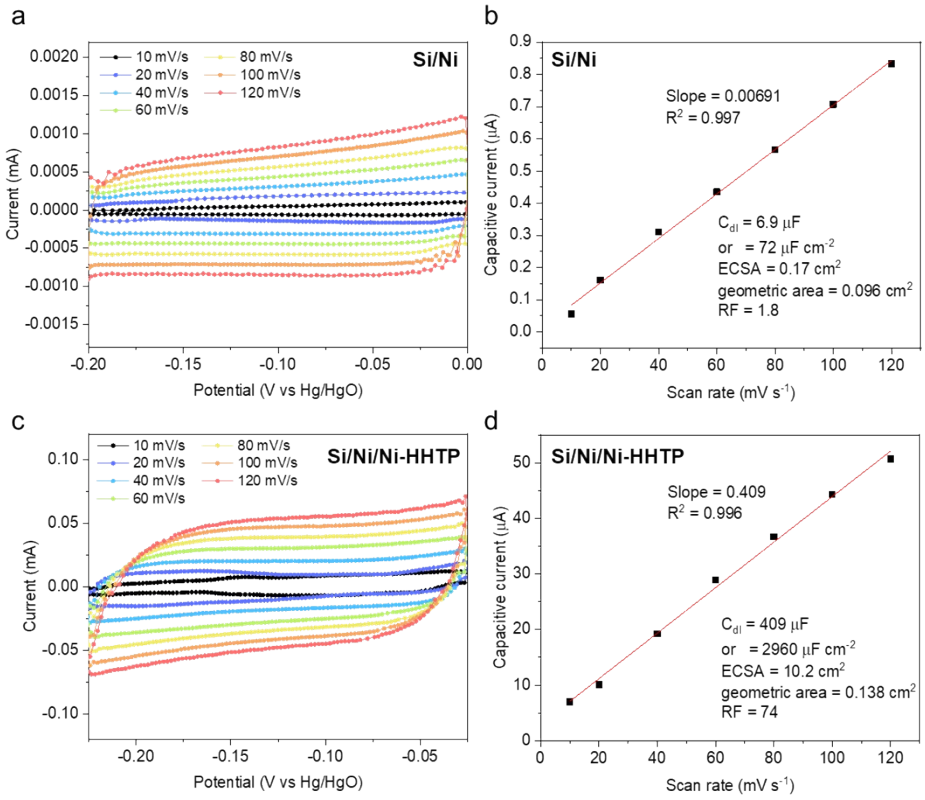

Figure S7. Electrochemical active surface area (ECSA) determination of Si/Ni and Si/Ni/Ni-HHTP Electrodes via double-layer capacitance measurements. CVs of (a) Si/Ni and (c) Si/Ni-HHTP at multiple scan rates (10-120 mV s^{-1}) in a non-Faradaic region in 1 M KOH. (b) Capacitive current vs. scan rate plot for Si/Ni, yielding a double-layer capacitance (C_{dl}) of 72 µF cm^{-2} and an ECSA of 0.17 cm^2. (d) Capacitive current vs. scan rate plot for Si/Ni/Ni-HHTP, yielding C_{dl} of 2960 µF cm^{-2} and an ECSA of 10.2 cm^2, demonstrating a significantly enhanced electrochemically active surface area compared to Si/Ni. Specific capacitance of 40 µF cm^{-2} of Ni surface in 1 M KOH was used to calculate ECSA.[5] The roughness factors (RF) was calculated by ECSA/geometric area.

Table S1. Comparison of double-layer capacitance (C_{dl}), electrochemical active surface area (ECSA) and geometric surface area of Si/Ni and Si/Ni/Ni-HHTP electrodes.

Electrode	C_{dl} (µF)	C_{dl} (µF cm^{-2})	ECSA (cm^2)	Geometric surface area (cm^2)	ECSA/ geometric area
Si/Ni	6.9	72	0.17	0.096	1.8
Si/Ni/Ni-HHTP	409	2960	10.2	0.138	74.1

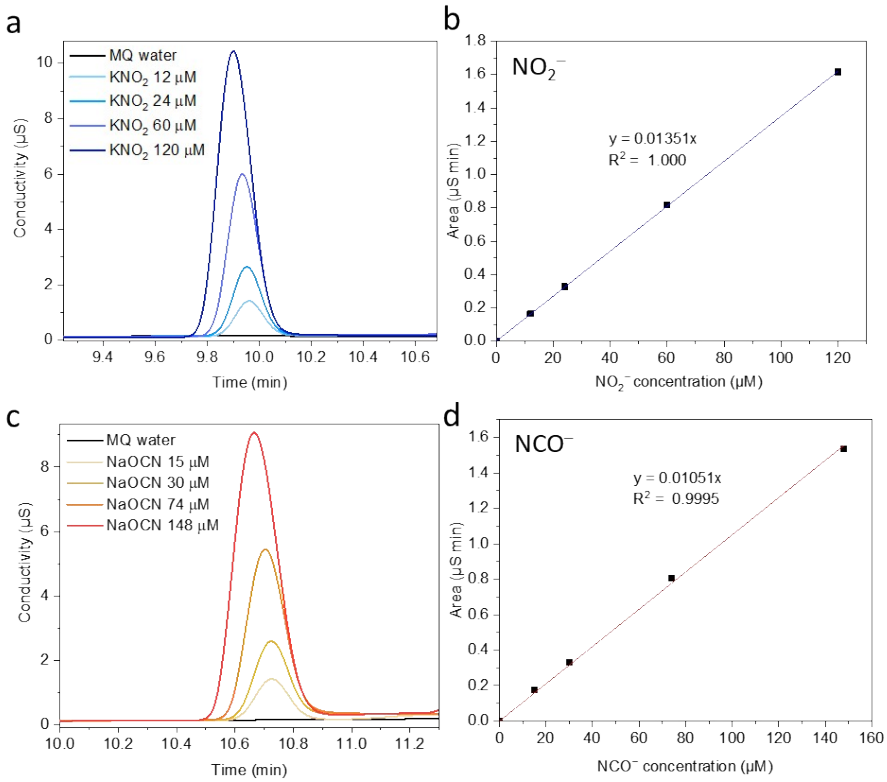

Figure S8. Ion chromatograms of standard solution of (a) NO_2^- and (c) NCO^-. Standard calibration curves of (b) NO_2^- and (d) NCO^-.

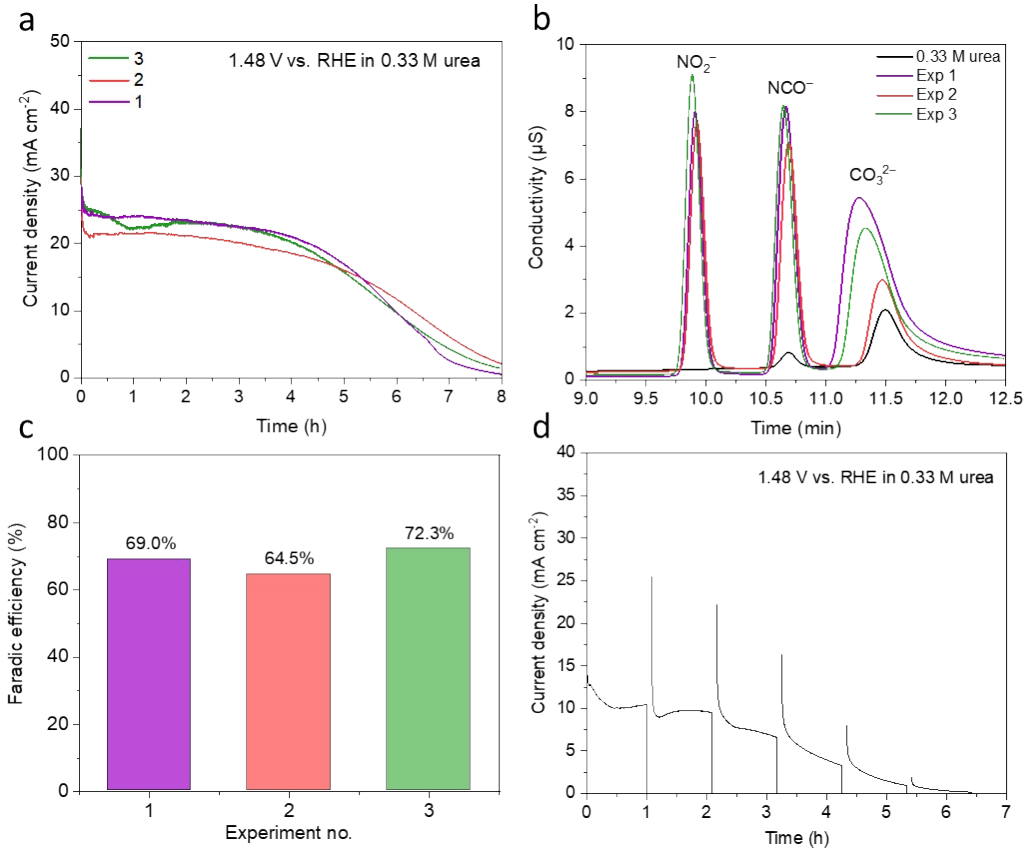

Figure S9. Product detection during UOR with three Si/Ni/Ni-HHTP electrodes. (a) CAs recorded at 1.48 V vs. RHE in 0.33 M urea + 1 M KOH solution (b) Ion chromatograms of the electrolyte after UOR reaction after 8 h of reaction. (c) Faradaic efficiency (%) based on NO_2^-. and (d) CAs recorded at 1.48 V vs. RHE in 0.33 M urea + 1 M KOH solution as a function of the electrolysis time.

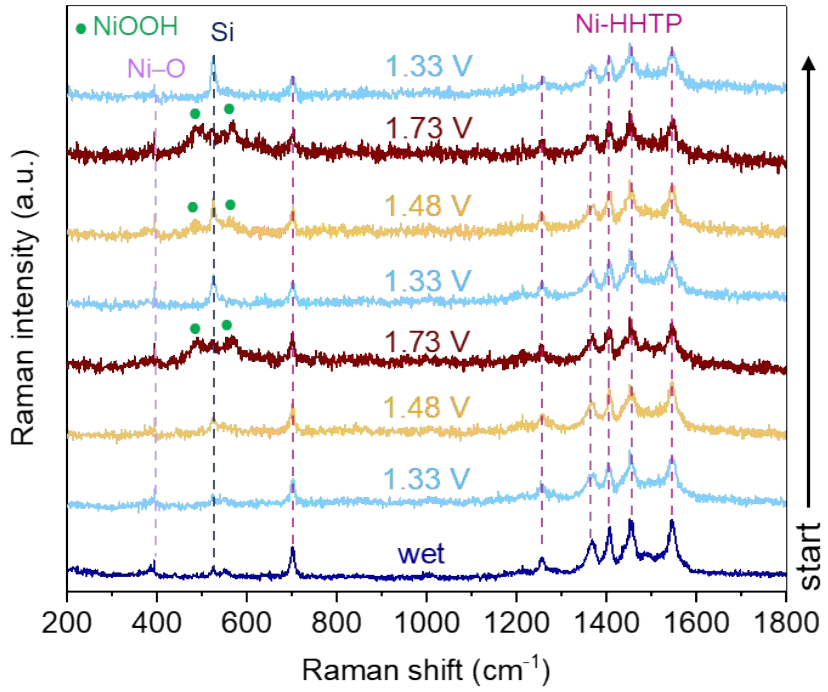

Figure S10. *In situ* Raman spectroscopy of Si/Ni/Ni-HHTP in 0.33 M urea + 1 M KOH at different potentials during two consecutive potential sweep cycles. The electrode was polarized 4 min at each potential.

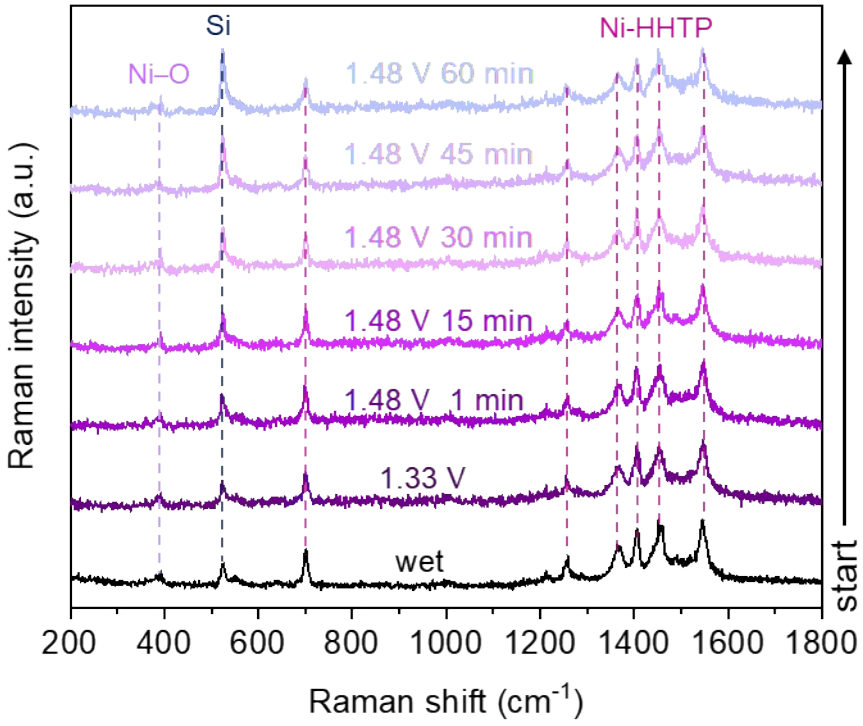

Figure S11. *In situ* Raman spectroscopy of Si/Ni/Ni-HHTP in 0.33 M urea + 1 M KOH at 1.48 V vs. RHE during 1 to 60 min.

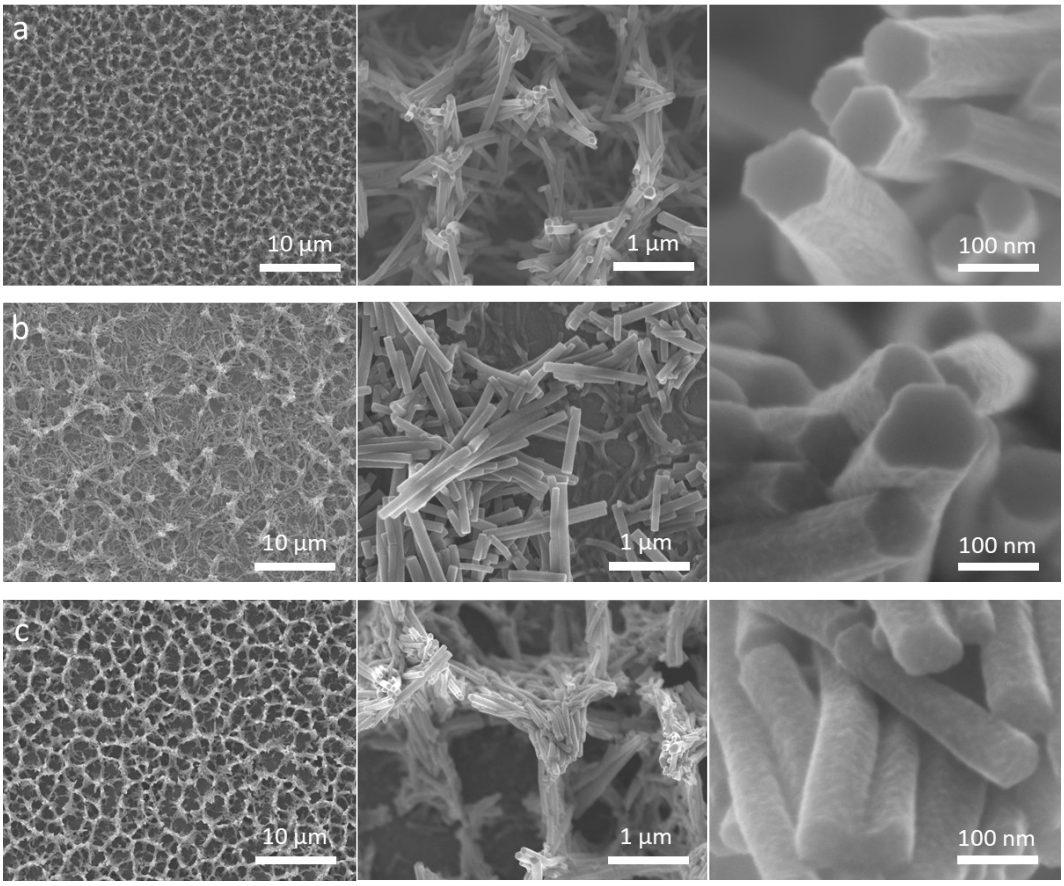

Figure S12. SEM images of Si/Ni/Ni-HHTP (a) as-prepared, (b) after OER and (C) after UOR.

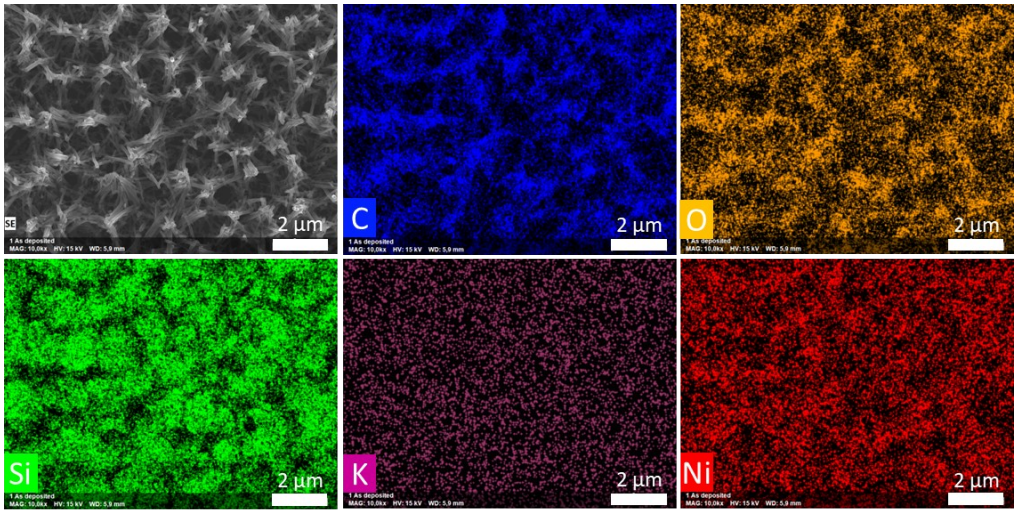

Figure S13. EDX mapping of as-prepared Si/Ni/Ni-HHTP.

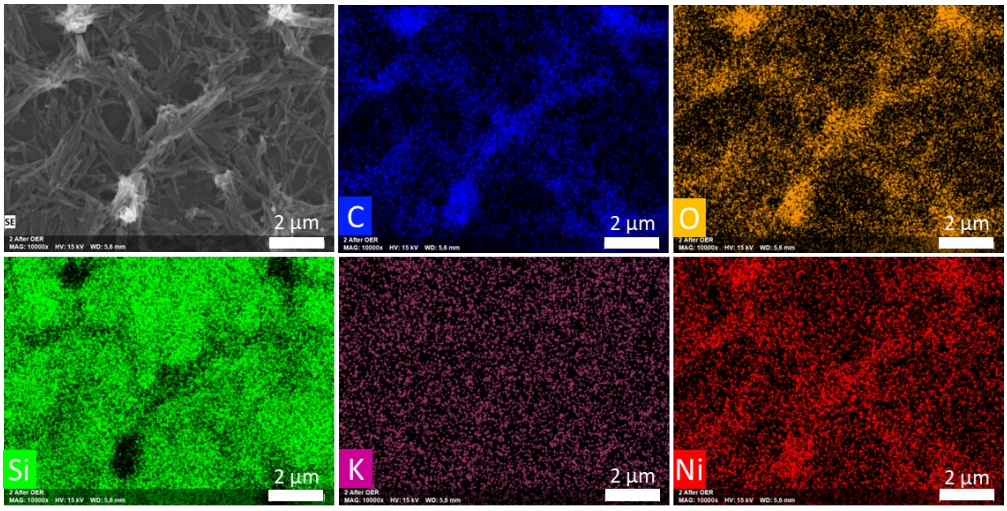

Figure S14. EDX mapping of Si/Ni/Ni-HHTP after OER.

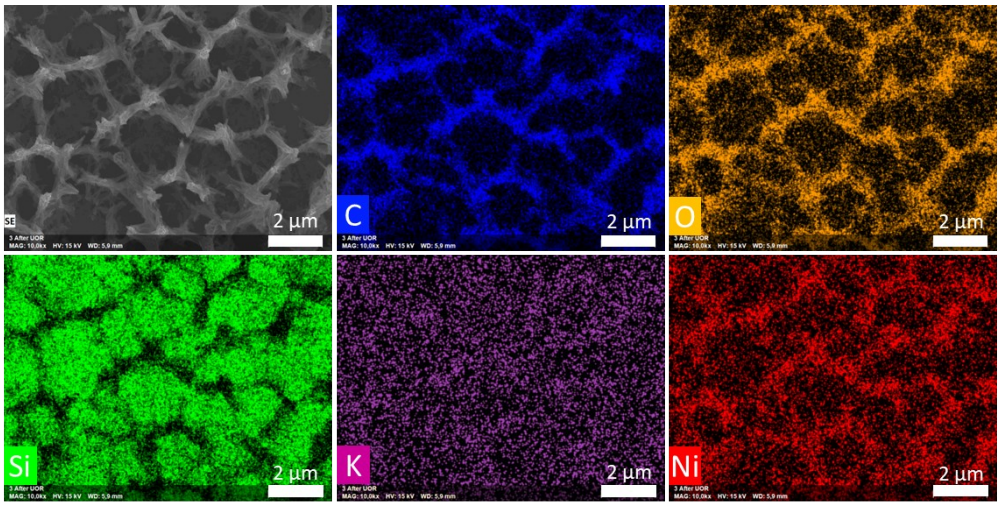

Figure S15. EDX mapping of Si/Ni/Ni-HHTP after UOR.

4. References

[1] R. Zniber, R. Achour, M. Z. Cherkaoui, B. Donnio, L. Gehringer and D. Guillon, *J. Mater. Chem.,* 2002, **12**, 2208-2213.
[2] F. C. Krebs, N. C. Schiodt, W. Batsberg and K. Bechgaard, *Synthesis,* 1997, 1285-1290.
[3] V. Percec, M. R. Imam, M. Peterca, D. A. Wilson, R. Graf, H. W. Spiess, V. S. K. Balagurusamy and P. A. Heiney, *J. Am. Chem. Soc.*, 2009, **131**, 7662-7677.
[4] G. Zhan, L. Hu, H. Li, J. Dai, L. Zhao, Q. Zheng, X. Zou, Y. Shi, J. Wang, W. Hou, Y. Yao and L. Zhang, *Nat. Commun.,* 2024, **15**, 5918.
[5] C. C. L. McCrory, S. Jung, J. C. Peters and T. F. Jaramillo, *J. Am. Chem. Soc.*, 2013, **135**, 16977–16987.